Parametric studies and reliability of near-wall turbulence modeling for Large Eddy Simulation of incompressible flows

*Khan Raqib Mahmud**
Department of Computer Science and Engineering,
University of Liberal Arts Bangladesh
Dhaka 1209, Bangladesh

M. M. Rhaman
Department of Mathematics, American International University-Bangladesh
Dhaka 1213, Bangladesh

Abul Kalam Al Azad
Department of Computer Science and Engineering,
University of Liberal Arts Bangladesh
Dhaka 1209, Bangladesh

**Corresponding Author*: *raqib.mahmud@ulab.edu.bd*

ABSTRACT

We present the parametric studies of near-wall turbulence modeling for Large Eddy Simulation (LES) of incompressible flows. Flow across a step channel is considered for the numerical studies as the complex wall bounded flows can be highly sensitive to the friction enforced and results are analyzed according to the physics of the flow. We apply the wall shear stress model to model the boundary layers in LES which we refer to as near-wall turbulence modeling. This paper is mainly concerned with the investigation of sensitivity of friction parameter of wall shear stress model and the reliability of near-wall turbulence modeling for LES of incompressible flows. The accuracy and efficiency of LES with near-wall turbulence modeling for complex turbulent flows are investigated by the parametric studies of model parameters. It is observed that wall shear stress model computes the reattachment length for flows in a step channel for both constant and parabolic inflow profile efficiently and with high accuracy compared with other results.

ISSN 1823- 5514, eISSN 2550-164X
Received for review:2016-10-20
Accepted for publication: 2017-07-19
Published: 2017-12-31

Keywords: *Near-wall turbulence modeling, Large Eddy Simulation, Reattachment length, Wall shear stress model, Slip with friction boundary condition.*

Introduction

For the simulation of turbulent flows, Large Eddy Simulation (LES) is one of the adequate techniques when dynamic features of the turbulent flows are needed [13]. This paper is mainly concerned with the investigation and development of near-wall turbulence modeling for LES of incompressible flows. The past decade has seen a promising development of the mathematical theory of LES of incompressible flows and in particular the investigation of Implicit LES models. In the frame of the General Galerkin method (G2) [7] the effect of unresolved scales is taken into account by an implicit subgrid model built from numerical stabilization of the finite element scheme.

The performance of the class of LES models is intrinsically limited by the numerical treatment of boundary walls. This remains a challenge due to the prohibitive computational cost as integrating the solution in the boundary layers requires mesh refinement and from a physical point of view as complex wall bounded flows can be highly sensitive to the friction enforced.

In this paper, we investigate the sensitivity of wall modeling with respect to model parameters in LES of incompressible turbulent flows in different geometries. Wall shear stress model [6] is used to model the turbulent boundary layers where the tangential velocity is prescribed with the shear stress model and a skin friction parameter chosen based on the Reynolds number and the roughness of the boundary. The performance of LES with near-wall turbulence modeling for complex turbulent flows are investigated by considering a constant and parabolic inflow profile across a step channel. The motivation to consider this case is that similar types of real engineering problems are very prevalent. We find that the wall model captures correctly the delayed separation and computes correctly the reattachment length for flows in a complex geometry. The sensitivity of the skin friction parameter of wall shear stress modeling on the flow field is studied and the results are analyzed according to the physics of the flow. Wall shear stress models that provide no slip, pure slip and slip with friction boundary conditions by parameter changing are employed with the LES. Numerical studies on two-dimensional channel flows across a step in two dimension using near-wall turbulence modeling are presented.

Large Eddy Simulation Technique

A new approach to computational turbulence modeling was introduced in [7], which is referred to as General Galerkin (G2) turbulence simulation. In the frame of G2 turbulence simulation, turbulence is modeled by weak solutions to the Navier–Stokes equations and a stabilized finite element method is used to compute approximations with a posteriori error control based on the error in the functional output.

Incompressible Homogeneous Navier-Stokes Equations

We consider the incompressible homogeneous Navier–Stokes equations as the basic model in which incompressibility expresses that the density ρ is a function of pressure $p, \rho = \rho(p)$ and does not change with pressure i.e. the Lagrangian derivative of ρ is equal to zero, $\frac{D\rho}{Dt} = 0.$ The homogeneity implies that the density is constant everywhere i.e. $\rho(.,t) = \text{constant}.$

The equations express conservation of momentum and conservation of mass or the continuity equation with incompressibility and isothermal i.e. constant temperature for a Newtonian fluid with viscous stresses depending linearly on velocity gradients and constant kinematic viscosity $\nu > 0$ enclosed in a volume $\Omega \subset \mathrm{R}^3$ over a time interval $\mathrm{I} = (0;T]$, where Ω is a polygonal:

$$\begin{aligned} \dot{u} + (u.\nabla)u - \nu\Delta u + \nabla p &= f, \qquad (x,t) \in \Omega \times I \\ \nabla . u &= 0, \qquad (x,t) \in \Omega \times I \\ u(x,0) &= u^0(x), \quad x \in \Omega \end{aligned} \tag{1}$$

where $u(x,t)$ is the velocity vector, $p(x,t)$ is the pressure, $u^0(x)$ is the initial data and $f(x,t)$ is the body force. The quantity $\nu\Delta u - \nabla p$ represents the total fluid force and can be expressed as:

$$\nu\Delta u - \nabla p = div\sigma(u,p)$$

where $\sigma(u,p) = (\sigma_{ij}(u,p))$ is the Cauchy stress tensor. The stress tensor $\sigma_{ij} = 2\nu\varepsilon_{ij}(u) - p\delta_{ij}$ with strain rate tensor $\varepsilon_{ij}(u) = 1/2(\partial u_i / \partial x_j + \partial u_j / \partial x_i)$ and δ_{ij} the Kronecker delta function, and the relative importance of viscous and inertial effects in the flow determined by the Reynolds number $\mathrm{Re} = \mathrm{UL}/\nu$, where U and L are characteristic velocity and length scales. If we assume that equation (1) is non-dimensionalized by the reference velocity U and typical length scale L

so that U and L are both equal to one, we get the Reynolds number Re is equal to ν^{-1}.

Boundary Conditions

A slip with friction boundary condition corresponds to setting the normal component of the velocity to zero at the solid boundary together with a friction condition on the tangential velocity. Such boundary conditions are more suitable for LES where large eddies of a turbulent flow are computed accurately, to describe the phenomena such as main vortices, move on the boundary (slip) and loose energy while moving (friction).

Weak Formulation

We define a pair of test functions $\hat{v} = (v, q) \in \hat{V}$ where $\hat{V}$ is a test function space defined by,

$$\hat{V} = \left\{ \hat{v} \in H^1(Q)^4 : v \in L_2(I; H_0^1(\Omega)^3) \right\}$$

over the space-time domain $Q = \Omega \times I$ where

$$L_2(I;\Omega) := \left\{ v : I \mapsto \Omega \middle| \int_\Omega v^2 < \infty \right\}$$

denotes the space of square-integrable Lebesgue functions. We choose ((. , .)) is the $L_2(Q)^m$ inner product with $m = 1,3$ or a suitable duality pairing over the space-time domain Q. The space

$$H^1(\Omega) := \left\{ v : \Omega \mapsto R \middle| v, \nabla v \in L_2(\Omega) \right\}$$

denotes the corresponding Sobolev space of functions that have square-integrable derivatives and $H_0^1(\Omega)$ is the Sobolev space of functions being zero on the boundary and square-integrable together with their first derivatives over $\Omega \subset R^3, \Omega \neq \Phi$ with boundary $\Gamma = \partial\Omega$, with dual $H^{-1}(\Omega)$.

Then the weak formulation of equation (1) can be obtained by multiplying (1) with the pair of test functions $\hat{v} = (v, q) \in \hat{V}$ and integrating over the domain Ω. So, the weak problem is to find $\hat{u} = (u, p)$ such that,

$$\int_{\Omega} \dot{u}\,.v + \int_{\Omega} (u\,.\nabla u).v + \int_{\Omega} \sigma : \nabla v - \int_{\Gamma\times I} \sigma v.nds - \int_{Q} f\,.v = 0$$

$$\int_{Q} \nabla.u\,.q = 0$$

Here **":"** denotes double dot product which is sum of the products over all components and all derivatives i.e., $\sigma : \nabla v = \sum_{i=1}^{i=3}\sum_{j=1}^{j=3} (\sigma)_{ij}(\nabla v)_{ij}$, $\int_{Q} u.v$ denotes $\int_{I}\int_{\Omega} u.vdxdt$, $\sigma(u,p) = \sigma_{ij} = 2\nu\varepsilon_{ij}(u) - p\delta_{ij}$ and the part $\int_{\Gamma\times I} \sigma v.nds = \int_{\Gamma\times I} (2\nu\varepsilon(u) - p\delta_{ij})v.nds = 0$ as we impose Neumann boundary conditions on one part of the boundary and $u = 0$ on the remaining part.
So the weak form becomes,

$$\int_{\Omega} \dot{u}\,.v + \int_{\Omega} (u\,.\nabla u).v + \int_{\Omega} \sigma : \nabla v - \int_{Q} f\,.v = 0$$

$$\int_{Q} \nabla.u\,.q = 0$$

We write this weak problem into the short form,

$$\begin{aligned}&((R(\hat{u}),\hat{v})) \equiv ((\dot{u},v)) + (((u.\nabla)u,v)) - ((\nabla.v,p)) + ((\nabla.u,q)) + \\ &((2\nu\varepsilon(u),\varepsilon(v))) - ((f,v)) = 0\end{aligned} \tag{2}$$

where $((u,v)) = \int_{I}\int_{\Omega} u.vdxdt.$

Time Discretization Scheme

A classical time-discretization scheme known as the -scheme known as the θ - scheme can be defined as

$$\frac{u^{n+1}-u^{n}}{\delta t} + \theta F(u^{n+1}) + (1-\theta)F(u^{n}) = f, \quad \theta \in [0,1] \tag{3}$$

for a scalar and liner problem:

$$\frac{\partial u}{\partial t} + F(u) = f$$

For $\theta = \frac{1}{2}$, the method (3) is an implicit method known as Crank–Nicolson method. The Crank–Nicolson method has an accuracy of order $O(\Delta t^2)$. Also for a convection dominated problem this method is unconditionally stable and does not have damping property. Now for the time discretization of the weak formulation (2) of the Navier–Stokes equations (1), we use Crank Nicolson method.

Let $0 = t_0 < t_1 < t_2 < \ldots < t_N = T$ be a sequence of discrete time steps with associated time intervals $I_n = (t_{n-1}, t_n)$ of length $k_n = t_n - t_{n-1}$, then the time discretization of the weak problem (2) is the following:

$$\begin{aligned}&((u^n - u^{n-1})k_n^{-1} + \hat{u}^n.\nabla\hat{u}^n, v) + (2\nu\varepsilon(\hat{u}^n), \varepsilon(v)) - (p^n, \nabla.v) + \\ &((\nabla.\hat{u}^n, q)) = (f, v)\end{aligned} \tag{4}$$

where $\hat{u}^n = \frac{1}{2}\left(u^n + u^{n-1}\right)$. This approach requires solving a nonlinear problem at each time step.

Space Discretization: Finite Element Method

For finite element space discretization of the weak form (4) of Navier–Stokes equations, we choose Lagrange P1/P1 elements (continuous linear velocity and pressure) which are equal order interpolation velocity–pressure elements.

We seek $\hat{U} = (U, P)$, continuous piecewise linear in space and time, and the space discretization for NSE (1) with homogeneous Dirichlet boundary conditions reads:

for $n = 1,2,\ldots\ldots, N$ find $(U^n, P^n) \equiv (U(t_n), P(t_n))$

with $U^n \in V_0^n \equiv [W_0^n]^3$ and $P^n \in W^n$ where $W^n \subset H^1(\Omega)$, such that

$$\begin{aligned}&((U^n - U^{n-1})k_n^{-1} + \hat{U}^n.\nabla\hat{U}^n, v) + (2\nu\varepsilon(\hat{U}^n), \varepsilon(v)) - (P^n, \nabla.v) \\ &+ ((\nabla.\hat{U}^n, q)) = (f, v) \forall \hat{v} = (v, q) \in V_0^n \times W^n\end{aligned} \tag{5}$$

Concerning the stability of the space discretization we see that this discretization is not stable since it does not satisfy the inf–sup stability condition. The stable and convergent choices for the finite element spaces are those which satisfy the following inf–sup or Babuska–Brezzi condition [8, 9, 12]:

$$\inf_{0\neq P^n\in W^n}\sup_{0\neq U^n\in V^n}\left\{\frac{(P^n,\nabla.U^n)_\Omega}{\left\|P^n\right\|_{L_0^2(\Omega)}\left\|U^n\right\|_{H^1(\Omega)}}\right\}\geq\gamma>0 \tag{6}$$

where γ is a constant independent of mesh size. Since the P1/P1 discretization is not compatible with the inf–sup condition, we can add certain stabilizing term to control spurious pressure oscillations to resolve the stability problem.

Stability and Consistency of Discretization Schemes

To avoid the problem of instability, we use a method in the context of finite element discretization that adds artificial viscosity using the Streamline Diffusion method. The idea of Streamline diffusion is to produce artificial diffusion acting only in the transport direction while maintaining the second order consistency of the scheme. This can be done by adding certain least square terms to the discretization.

Time Stepping Stability

Time stepping is important for the numerical stability and to resolve the turbulent motions accurately in time. The CFL condition which is applied in our simulation method, for the time step Δt is:

$$\Delta t<\Delta t_c=CFL\frac{\Delta x}{U_c} \tag{7}$$

where Δx is the cell size in the x direction, U_c is a convective velocity and CFL is the maximum allowable courant number that depends on the numerical scheme used. The finite element discretization of the Navier–Stokes equation (1) consists of a nonlinear term into the stiffness matrix so a system of nonlinear equations has to be solved. To solve the system of nonlinear equations Picard fixed point iteration method is used.

Streamline Diffusion Stability

We add certain least square terms to the finite element discretization (5) for the streamline-diffusion stability i.e. add a diffusion term acting only in the direction of the streamlines that gives a good stability and high accuracy [10, 11], then the discretization is [7]:

$$((U^n - U^{n-1})k_n^{-1} + \hat{U}^n.\nabla\hat{U}^n, v) + (2\nu\varepsilon(\hat{U}^n), \varepsilon(v)) -$$
$$(P^n, \nabla.v) + (\nabla.\hat{U}^n, q) + SD_\delta^n(\hat{U}^n, P^n; v, q) = (f, v) \quad (8)$$
$$\forall\hat{v} = (v, q) \in V_0^n \times W^n$$

where $\hat{U}^n = \frac{1}{2}\left(U^n + U^{n-1}\right)$ and P^n are piecewise constant in time over I_n with the stabilizing term

$$SD_\delta^n(\hat{U}^n, P^n; v, q) \equiv (\delta_1(\hat{U}^n.\nabla\hat{U}^n + \nabla P^n - f), \hat{U}^n.\nabla v + \nabla q)$$
$$+ (\delta_2\nabla.\hat{U}^n, \nabla.v) \quad (9)$$

and $(u, v) = \sum_{K\in T}\int_K v.w dx$ with the stabilization parameters

$$\delta_1 = K_1(k_n^{-2} + \left|U^{n-1}\right|^2 h_n^{-2})^{-1/2}$$
$$\delta_2 = K_2 h_n \quad (10)$$

where K_1 and K_2 are positives constants of unit order. For turbulent flow the size of the time step is chosen as:

$$k_n \sim \min_{x\in\Omega}(h_n / |U^{n-1}|) \quad (11)$$

so that

$$\delta_1 \sim k_n \sim \min_{x\in\Omega}(h_n / |U^{n-1}|)$$

Near-Wall Turbulence Modelling and Implementation

Wall shear stress model, a near wall modeling for turbulent wall layer of turbulent flows in a complex geometries can be written in the following form: If we divide a bounded domain $\Omega \subset \mathrm{R}^d$ with $d = 2,3$ into the boundaries $\partial\Omega = \Gamma_{\text{infl}} \bigcup \Gamma_{slfpr} \bigcup \Gamma_{\text{outfl}}$ so that the parts are mutually disjoint, then the slip with linear friction and penetration with resistance boundary conditions are applied on Γ_{slfpr} can be defined by:

$$u.n + \alpha n^T \sigma n = 0, \quad \text{on} \quad \Gamma_{slfpr} \quad (12)$$

$$u.\tau_k + \beta^{-1} n^T \sigma\tau_k = 0, \quad \text{on} \quad \Gamma_{slfpr} \quad 1 \le k \le d-1 \quad (13)$$

where σ is the shear stress, n is an outer normal vector on $\partial\Omega$, τ_k orthogonal unit tangent vectors at the boundary, α a penetration parameter and β a skin friction parameter are piecewise constant on the boundary Γ_{slfpr} and is chosen based on the Reynolds number and the roughness of the boundary also as a function of space and time similar to simple wall shear stress models [4, 5].

If we consider $\alpha \to 0$, we get no penetration condition and $\alpha \to \infty$ gives free penetration condition. If we choose no penetration condition into (12), then the condition $\beta \to 0$ in (13) gives free slip boundary conditions and $\beta \to \infty$ prescribes no slip conditions. We consider no penetration condition:

$$u.n = 0, \qquad \text{on} \quad \Gamma_{slfpr} \tag{14}$$

$$u.\tau_k + \beta^{-1} n^T \sigma \tau_k = 0, \qquad \text{on} \quad \Gamma_{slfpr} \quad 1 \le k \le d-1 \tag{15}$$

The slip boundary condition on Γ_{slfpr} describes that the normal velocity is zero on the boundary *i.e.* the pressure is the only nonzero flux on the given boundary Γ_{slfpr}. The tangential components (friction) *i.e.* slip with friction boundary condition in (15) is implemented in the weak form by adding boundary integrals in the variational form (2). So the weak form with the boundary integrals is:

$$\begin{aligned} &\int_Q \dot{u}\,.v + \int_Q (u\,.\nabla u).v + \int_Q \sigma\,\nabla.v - \int_{\Gamma_{slfpr}\times I} \sigma v.n - \int_Q f\,.v = 0 \\ &\int_Q \nabla.u\,.q = 0 \end{aligned} \tag{16}$$

where $\int_{\Gamma_{slfpr}\times I} \sigma v.n = \int_{\Gamma_{slfpr}\times I} \sigma v.n ds dt.$ We decompose the test function v on Γ_{slfpr} into d orthonormal components:

$$v = (v.n)n + \sum_{k=1}^{d-1} (v.\tau_k)\tau_k \tag{17}$$

Then the boundary integral in the variational formulation can be rewritten:

$$\int_{\Gamma_{slfpr}\times I} \sigma n.v = \int_{\Gamma_{slfpr}\times I} n^T \sigma n(v.n) + \int_{\Gamma_{slfpr}\times I} \sum_{k=1}^{d-1} n^T \sigma \tau_k (v.\tau_k)$$

Then implementing the normal and the tangential components of boundary conditions from equations (12) and (13) we rewrite the variational formulation of the boundary integral:

$$\int_{\Gamma_{slfpr}\times I} \sigma n.v = \int_{\Gamma_{slfpr}\times I} \alpha^{-1}(u.n)(v.n) - \int_{\Gamma_{slfpr}\times I} \sum_{k=1}^{d-1} \beta(u.\tau_k)(v.\tau_k)$$

Applying the normal and the tangential components condition, the weak form (16) with the boundary integrals is:

$$\int_Q \dot{u}\,.v + \int_Q (u\,.\nabla u).v + \int_Q \sigma\ \nabla.v -$$

$$\int_{\Gamma_{slfpr}\times I} \alpha^{-1}(u.n)(v.n) + \int_{\Gamma_{slfpr}\times I} \sum_{k=1}^{d-1} \beta(u.\tau_k)(v.\tau_k) - \int_Q f.v = 0$$

$$\int_Q \nabla.u\,.q = 0$$

The time and space discretization of this weak form with the boundary integrals where slip with friction boundary condition and penetration with resistance applied can be written in the following form from the equation (5):

$$((U^n - U^{n-1})k_n^{-1} + \hat{U}^n.\nabla\hat{U}^n, v) + (2\nu\varepsilon(\hat{U}^n), \varepsilon(v)) - (P^n, \nabla.v)$$
$$+ (\nabla.\hat{U}^n, q) - \int_{\Gamma_{slfpr}\times I} (\sigma(U^n, P^n).n).v\,ds = (f, v) \quad \forall\hat{v} = (v, q) \in V_0^n \times W^n$$

Implies

$$((U^n - U^{n-1})k_n^{-1} + \hat{U}^n.\nabla\hat{U}^n, v) + (2\nu\varepsilon(\hat{U}^n), \varepsilon(v)) - (P^n, \nabla.v) +$$
$$(\nabla.\hat{U}^n, q) - \int_{\Gamma_{slfpr}\times I} \alpha^{-1}(\hat{U}^n.n)(v.n) + \int_{\Gamma_{slfpr}\times I} \sum_{k=1}^{d-1} \beta(\hat{U}^n.\tau_k)(v.\tau_k)ds =$$
$$(f, v) \quad \forall\hat{v} = (v, q) \in V_0^n \times W^n$$

where $V_0^n \times W^n$ is defined in space discretization. If we consider no penetration conditions, then the boundary integral with penetration parameter vanishes and pure slip condition and slip with friction boundary conditions remain only, that we focused on here. For the strong implementation of Wall Shear Stress Model, the normal component condition *i.e.* slip boundary condition (14) is applied after assembling the stiffness matrix and the right-hand side vector (called load vector) by modifying the algebraic system. To modify the algebraic system, the row of the stiffness matrix and load vector corresponding to a boundary vertex is replaced by a new row according to the boundary condition, implemented according to [6].

Numerical Studies for Flow across a Step Channel

For flows in a step channel, the upstream boundary layer detaches at the sharp corner which forms a free shear layer. The transition begins soon after the detachment if the boundary layer is laminar. The separated shear layer curves sharply downward in the reattachment zone and collides on the wall, and part of the shear layer fluid is deviated upstream into the recirculating flow by a strong adverse pressure gradient.

For flows in a two-dimensional channel with a step, recirculating vortex appears behind the step and we compute the reattachment length of the recirculating vortex. The tangential velocity on the bottom boundary of the step channel does not disappear because of the boundary conditions specified, so the reattachment point can be defined by the change of the sign of the tangential velocity in which tangential velocity is negative to left of the reattachment point and positive to the right [1].

The geometry of the domain of a two dimensional channel flow across a step is used in the computation presented in Figure 1. The same domain was used in computations in [2] in order to simulate the experiments of separated Stokes flow by Taneda [3].

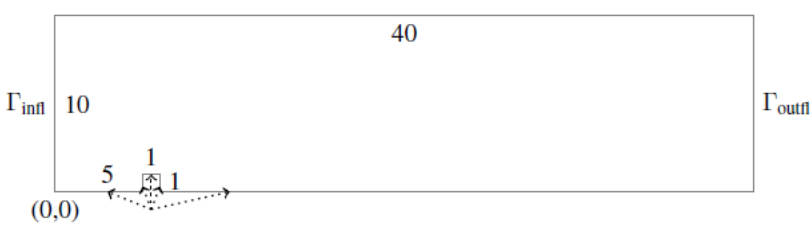

Figure 1: Geometry for a two-dimensional channel with a step

An inflow boundary condition specified on the left boundary Γ_{infl} of the domain, an outflow boundary condition Γ_{outfl} where the flow leaves which we say a "do nothing" boundary on the right boundary of the domain, a slip with friction boundary condition on the top and on the bottom boundary of the domain different boundary conditions are prescribed as different test case: no slip boundary condition, perfect slip boundary condition and slip with skin friction boundary condition, Figure 1.

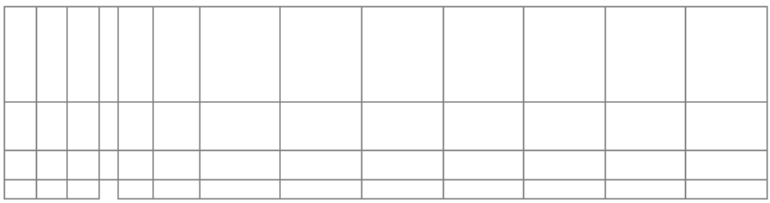

Figure 2: Computational grids (level 0) for a two-dimensional channel with a step

The results for a parabolic and a constant inflow profile as the inflow boundary conditions are analyzed. We performed our simulations with the initial grid (level 0) presented in Figure 2, similar to the grid presented in [1] taking the result as a benchmark.

Table1: Degrees of Freedom for Flow across a Step Channel

Level	Total Number
0	140
3	6818
4	26690
5	105602

The resulting degrees of freedom for finer levels are given in Table I. The higher levels of computational grid are generated by the dolphin mesh generation where initially level 0 grids are used as an input and in our simulation, we have used the method which is not adaptive.

To investigate the accuracy and efficiency of near-wall turbulence modeling for LES, we compute the reattachment point of recirculating vortex behind the step of the channel for different values of skin friction parameter β, we choose $\beta = \{0.0, 0.01, 0.05, 0.1, 0.5, 50.0, 100.0\}$. The choice of β, $\beta \to 0$ prescribes perfect slip boundary conditions and $\beta \to \infty$ no slip

boundary condition. The Reynolds number is taken based on the velocity at the inlet and height of the cube, $\mathrm{Re} = \frac{uh}{\nu}$, to compare our results with the results of other existing results. We performed the computations for i) viscosities $\nu = 0.01$ and $\nu = 0.02$, ii) inflow profile and iii) grid levels 3, 4 and 5.

We do the parametric studies to learn the sensitivity of near-wall turbulence modeling for LES by studying the effect of skin friction parameter to the reattachment point. For the reliability, we compare our results from the simulations with the existing numerical results, taken as a benchmark.

Parabolic Inflow Profile

The computations are performed for the parabolic inflow profile $\mathrm{u} = (u_1, u_2)^T$, with $u_1 = y(10-y)/25, u_2 = 0$ on Γ_{infl} of the step channel. Streamlines of a two-dimensional step channel are presented in Figure 3 for viscosity $\nu = 0.01$ and $\nu = 0.02$ for parabolic inflow and grid level 4.

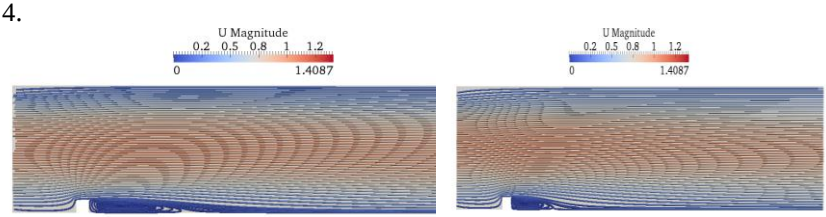

(a) For $\nu = 0.01$ (b) For $\nu = 0.02$

Figure 3: Velocity Streamlines of flow in a two-dimensional channel with a step for $\beta = 0.1$

In figure 4, we show the tangential velocity on the bottom wall for viscosity $\nu = 0.01$ and for parabolic inflow.

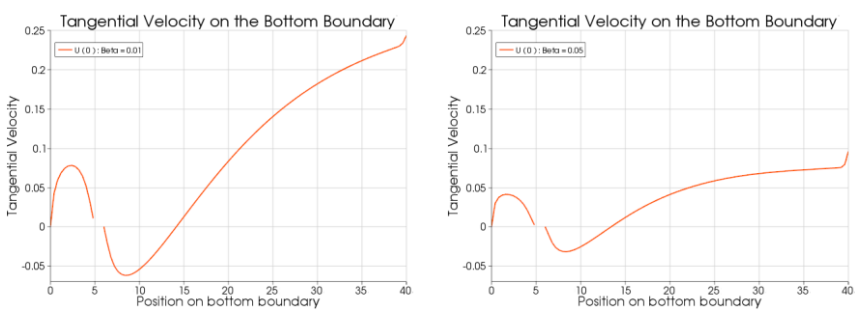

(a) For $\beta = 0.01$ (b) For $\beta = 0.05$

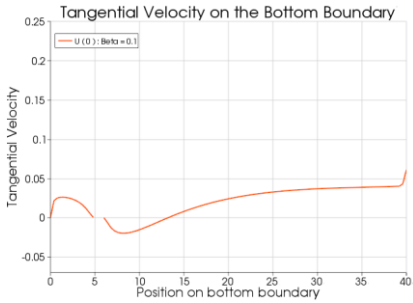

(c) For $\beta = 0.1$

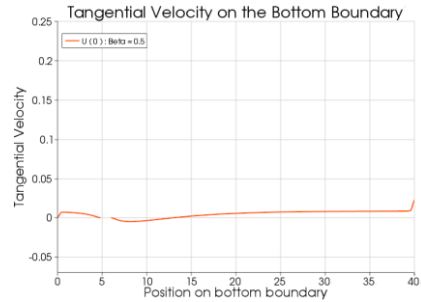

(d) For $\beta = 0.5$

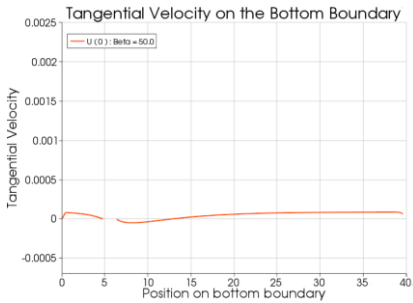

(e) For $\beta = 50$

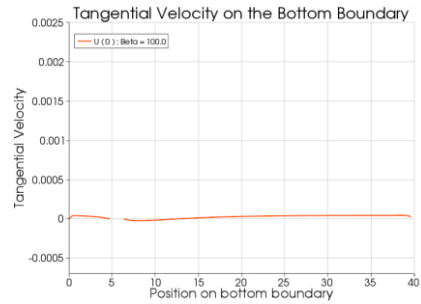

(f) For $\beta = 100$

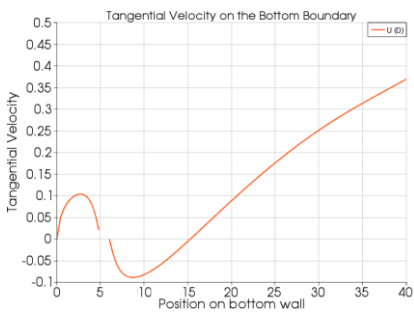

(g) For $\beta = 0$

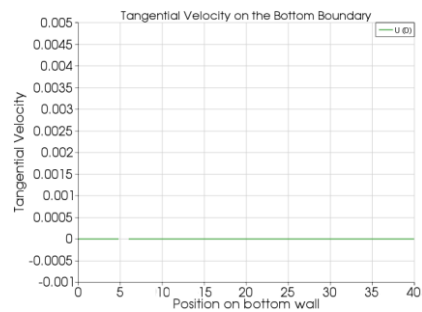

(h) For $\beta = \infty$

Figure 4: Tangential velocity for $\nu = 0.01$ and grid level 4

The figure 5 shows the tangential velocity for viscosity $\nu = 0.02$ on the bottom wall.

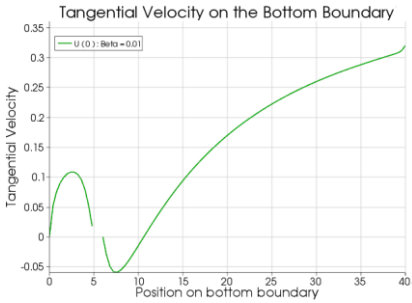

(a) For $\beta = 0.01$

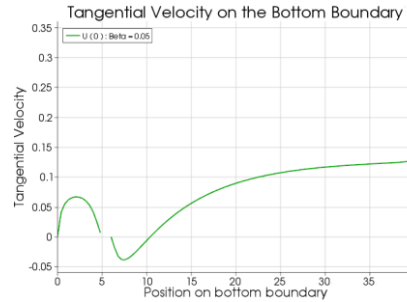

(b) For $\beta = 0.05$

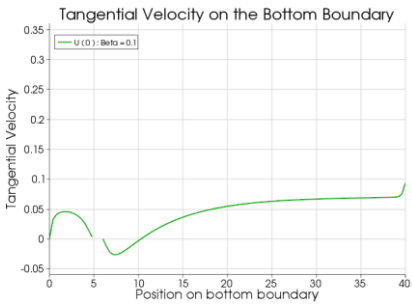

(c) For $\beta = 0.1$

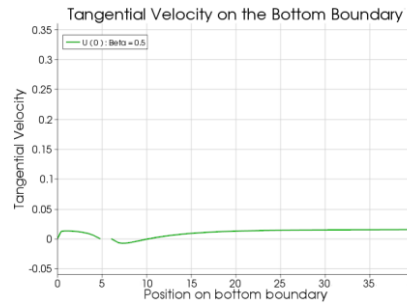

(d) For $\beta = 0.5$

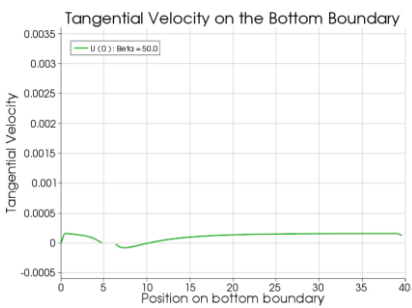

(e) For $\beta = 50$

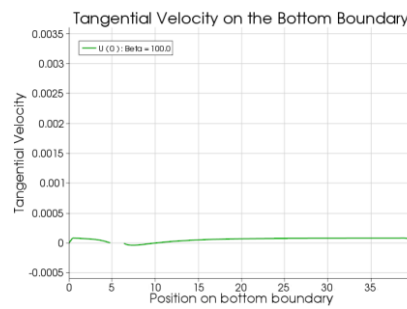

(f) For $\beta = 100$

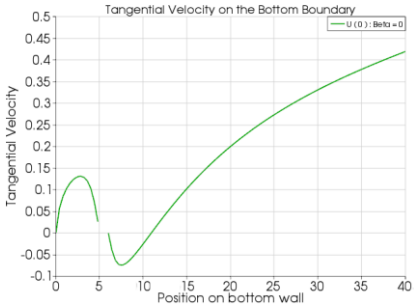

(g) For $\beta = 0$

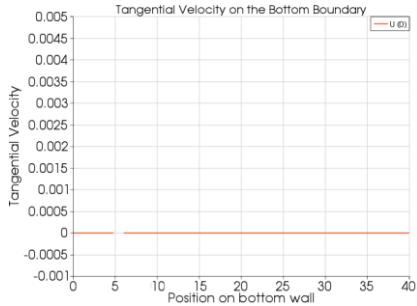

(h) For $\beta = \infty$

Figure 5: Tangential velocity for $\nu = 0.02$ and grid level 4

In figure 4 and 5 we observe that the tangential velocity decreases if the value of skin friction parameter β increases. From figures 4h and 5h, we see that the tangential velocities along the bottom wall of the step channel are zero for the no slip boundary condition

The reattachment points for viscosities $\nu = 0.01$ and $\nu = 0.02$, for different skin friction parameters and for different grid levels are presented into the plots 6a and 6b. We also presented the results from Volker John's numerical tests [1] in the same figures to have a comparison with our results.

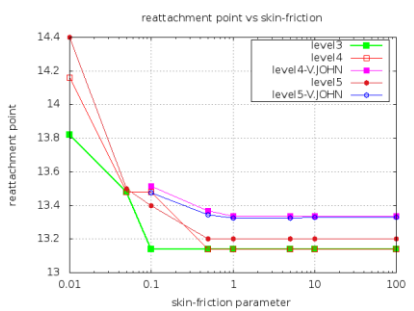

(a) For viscosity $\nu = 0.01$

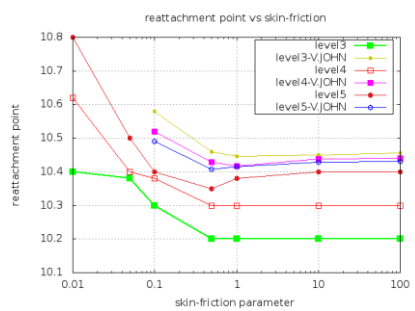

(b) For viscosity $\nu = 0.02$

Figure 6: Reattachment point of a two-dimensional step channel at different skin friction parameter for parabolic inflow profile

Remarks I

It is evident from Figures 6a and 6b that the reattachment length of the re-circulating vortex of $\nu = 0.02$ is smaller than that of $\nu = 0.01$. Further, it is observed that for both $\nu = 0.02$ and $\nu = 0.01$, the position of the reattachment

point moves towards the outflow boundary with the decreasing skin friction parameter $\beta \in \{0.0, 0.01, 0.05, 0.1, 0.5\}$ on the boundary.

The position of reattachment point is found to remain stationary close to the step of the channel for the friction parameter values $\beta \in \{0.0, 0.01, 0.05, 0.1, 0.5\}$. But for grid level 5 for $\nu = 0.02$, the position of the reattachment point is observed to advance closer towards the step with decreasing β, whereas with increasing β from a certain value, the position of the reattachment point remains stationary. So, the position of the reattachment point reaches to a local minimum for a certain value of β.

From Figures 6a and 6b, the positions of the reattachment points for different values of skin friction parameter β are found to be smaller than the numerical tests of Volker John [1] as this study uses G2 turbulent simulation technique as the governing numerical scheme. Moreover, G2 turbulent simulation technique is relatively more diffusive as this scheme uses streamline diffusion for numerical stabilization. Moreover, as regards to the Finite Element Discretization (FEM), P1/P1 discretization scheme is implemented in the current study, whereas in [1] Q2/P1 scheme was used in the numerical analysis. Consequently, the number of degrees of freedom required in this study is considerably less than that in [1].

It is also observed from the Figures 6a and 6b that, the values of the stabilizing parameter of finer grid level are smaller than that of the coarser level resulting that the position of the reattachment point for finer grid level is higher than that of coarser level as the numerical scheme is less diffusive. It may be noted that for small values of the skin friction parameter the position of the reattachment point moves in all computations towards the outflow boundary; therefore, these values are not explicitly shown. Also, the position of the reattachment point for large values of the skin friction parameter on a coarse level is too close to the no slip boundary conditions to catch on a fine level [1]. This is implied in Figures 4h and 5h as the absence of tangential velocity for no-slip boundary condition.

From Figures 4 and 5, it is observed that the tangential velocity decreases with increasing the skin friction parameter β values, and for the very high values of β the tangential velocity tends to zero which rather behaves like a no slip boundary condition. Also in Figures 4g and 5g, that the tangential velocity of using the perfect slip ($\beta = 0$) boundary condition is observed to be bigger than the tangential velocity of using slip with friction boundary condition and a bigger reattachment length is observed.

Constant Inflow Profile

Results for computations are presented when constant inflow profile $u_1 = 1, u_2 = 0$ is used on the inlet. Streamlines of a two dimensional step

channel for constant inflow are presented in Figure 7 for viscosity $\nu = 0.01$, $\nu = 0.02$ and for grid level 4.

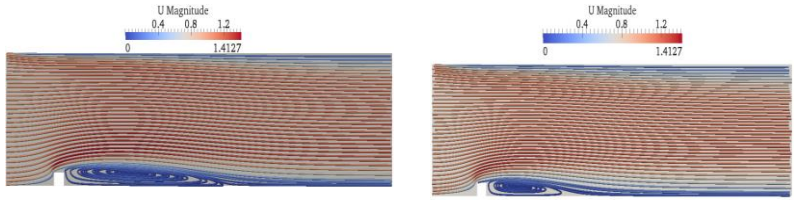

(a) For $\nu = 0.01$ (b) For $\nu = 0.02$

Figure 7: Velocity Streamlines of flow in a two dimensional channel with a step for $\beta = 0.1$

The Figure 8 shows the tangential velocity on the bottom wall for viscosity $\nu = 0.01$.

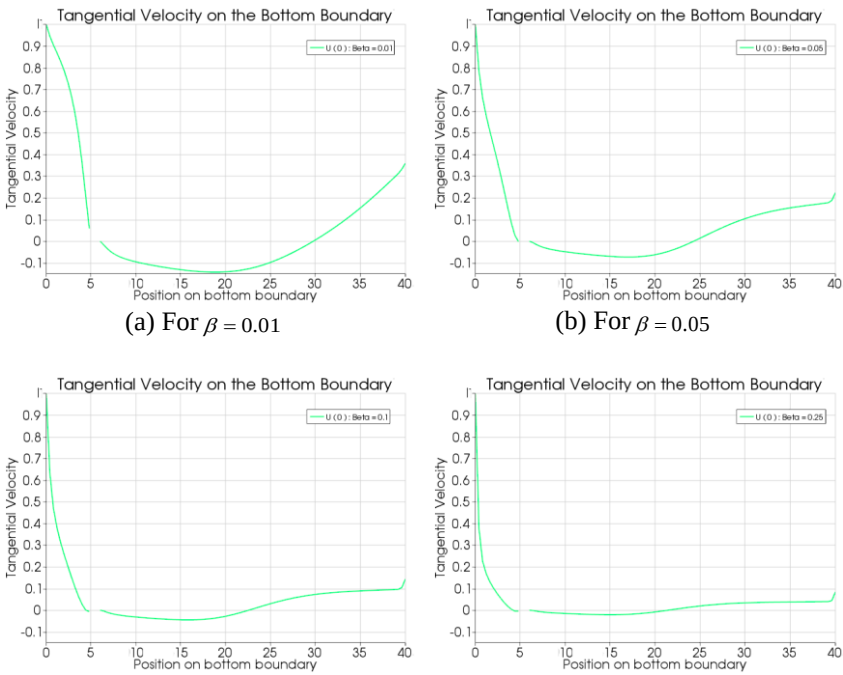

(a) For $\beta = 0.01$ (b) For $\beta = 0.05$

(c) For $\beta = 0.1$ (d) For $\beta = 0.25$

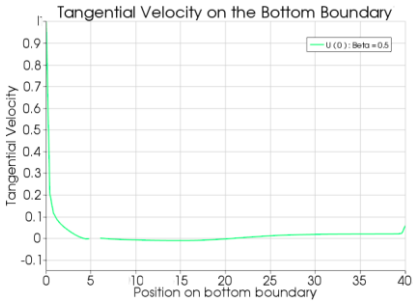

(e) For $\beta = 0.5$

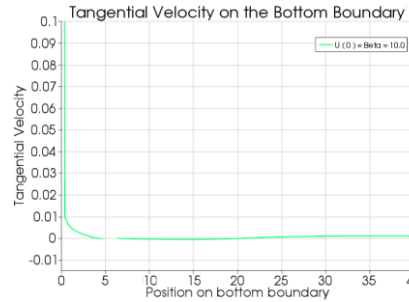

(f) For $\beta = 10$

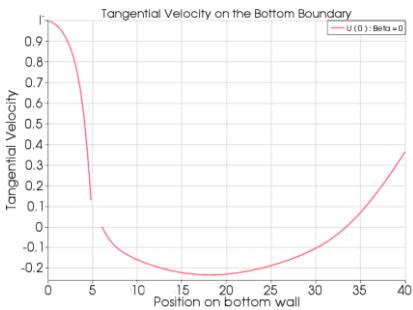

(g) For $\beta = 0$

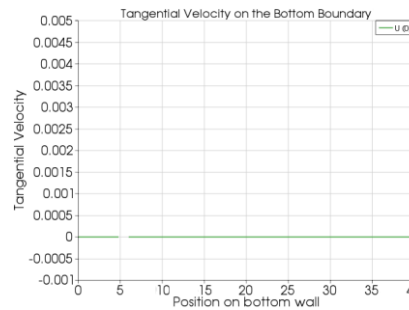

(h) For $\beta = \infty$

Figure 8: Tangential velocities for $\nu = 0.01$ and for grid level 4

Tangential velocities for viscosity $\nu = 0.02$ are presented into the Figures 9.

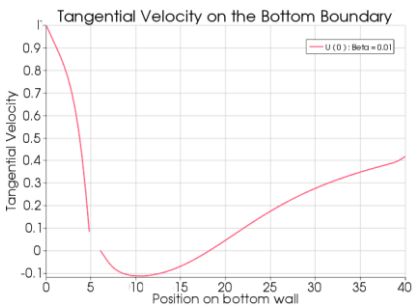

(a) For $\beta = 0.01$

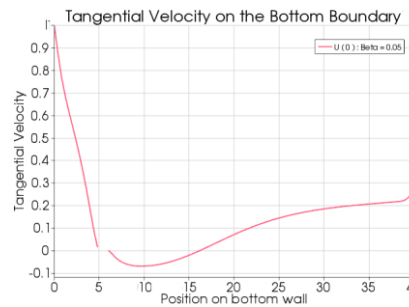

(b) For $\beta = 0.05$

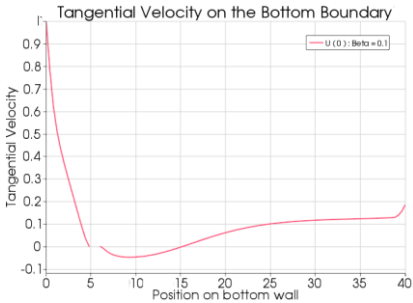

(c) For $\beta = 0.1$

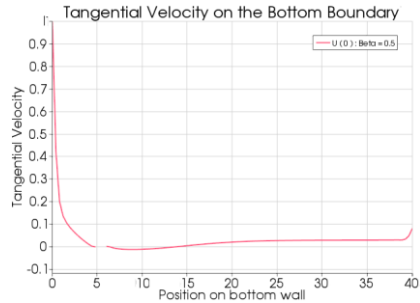

(d) For $\beta = 0.5$

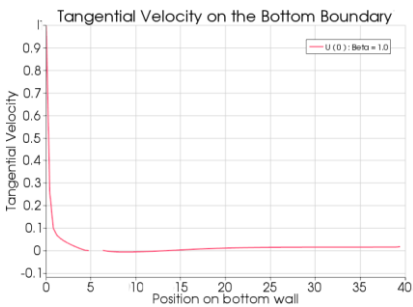

(e) For $\beta = 1.0$

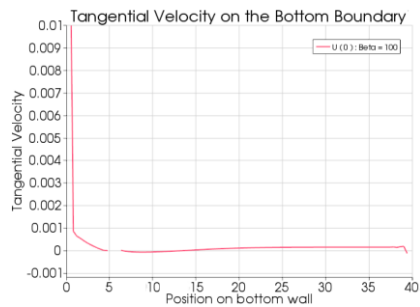

(f) For $\beta = 100$

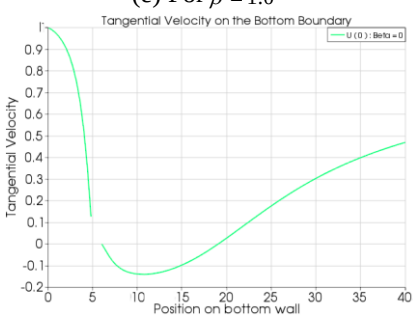

(g) For $\beta = 0$

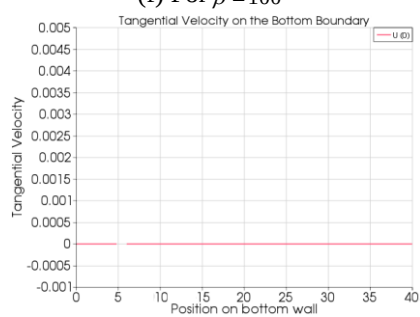

(h) For $\beta = \infty$

Figure 9: Tangential velocities for $\nu = 0.02$ and for grid level 3

From the figures 8 and 9, it is observed that the tangential velocity along the bottom wall decreases if the values of skin friction parameter increase. Positions of reattachment points for viscosity $\nu = 0.01$ and $\nu = 0.02$, for different values of skin friction parameters and for different grid levels are

presented into the figures below 10a and 10b, also the results of the numerical tests from Volker John [1].

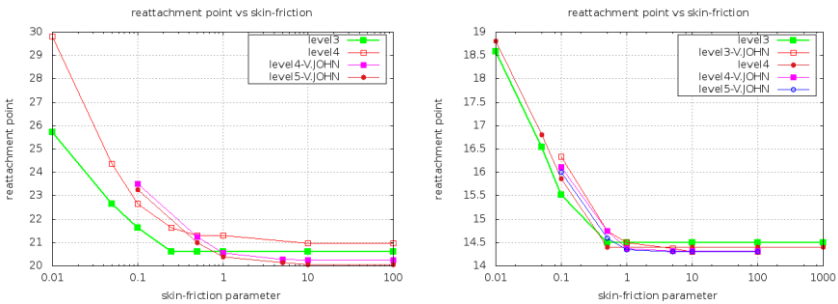

(a) For $\nu = 0.01$ (b) For $\nu = 0.02$

Figure 10: Reattachment point of a two-dimensional step channel at different skin friction parameter for constant inflow profile

Remarks II

From Figures 10a and 10b, it is observed that the reattachment length of the recirculating vortex of $\nu = 0.02$ is smaller than that of $\nu = 0.01$. Moreover, the position of the reattachment point is found to move towards the outflow boundary with decreasing the skin friction parameter β on the boundary, and the position of reattachment point remains stationary and close to the step for $\beta \in \{0.5, 0.1, 10, 100\}$.

For viscosity $\nu = 0.01$, for grid level 4, the position of the reattachment point moves towards the outflow boundary for smaller values of skin friction parameter. In Figures 10a and 10b, comparing the results with the results of Volker John numerical tests [1], it is observed that for smaller values of β , the current simulation results smaller values of positions of reattachment point because of stabilized numerical scheme.

From Figures 8 and 9, it is further evident that the tangential velocity decreases if the value of the skin friction parameter β increases and from Figures 8h and 9h, it is observed that for the very high values of β the tangential velocity tends to zero which behaves like a no slip boundary condition. Furthermore, Figures 8g and 9g show the tangential velocity, by using the perfect slip boundary condition, is bigger than the tangential velocity by using slip with friction boundary condition and also this yields a bigger reattachment length.

Conclusion

For the Large Eddy Simulation to characterize the small scale features there is a great importance of how well we can treat the boundary layers. To treat the turbulent boundary wall we used Wall Shear Stress model and analyzed the effect of the friction parameters of that model with different boundary conditions. We studied the dependency of position of this reattachment point on the value of the model parameter of near wall turbulence modeling. We observe that the Wall Shear Stress model can compute the reattachment length for both constant and parabolic inflow profile efficiently as our model only incorporates parametric values for different boundary conditions of inflow profile whereas other models involve different boundary model for the computation of the near wall flow. It also can be mentioned that near wall turbulence model computes the reattachment length with high accuracy comparing with others. It is also observed that the wall boundary model is able to characterize the turbulent flow features. There is scope for the future work to perform the simulation with the Delayed Deatched Eddy Simulation (DDES) wall model and then compare the results with the Wall Shear Stress Model. We note that the choice of model parameters depends on the computational mesh, time step, the solution itself and the problem data. Also the choice of skin friction parameter is not certain, so there is scope to work on the uncertainty quantification of the skin friction parameter.

References

[1] Volker John. "Slip with friction and penetration with resistance boundary conditionds for the Navier-Stokes equations-numarical tests and aspects of the implementation." Journal of Computational and Applied Mathematics. Volume-147, 2002.

[2] V. P. Fragos, S. P. Psychoudaki and N. A. Malamataris. "Computer aided analysis of flow past a surface mounted obstacle." International journal for numerical methods in fluids. Volume-25, 1997.

[3] S. Taneda. "Visualization of separating Stokes flows." Phys. Soc. Jpn., Volume-46, 1979.

[4] U. Schumann. "Subgrid Scale Model for Finite Difference Simulations of Turbulent Flows in Plane Channels and Annuli." Journal of Computational Physics. Volume-18, 1975.

[5] Ugo Piomelli and Elias Balaras. "Wall-Layer Models for Large-Eddy Simulations." Annu. Rev. Fluid Mech., Volume-34, 2002.

[6] M. Nazarov. "Algorithms and Higher Order Stabilization for Finite Element Computation of Turbulent Compressible Flow.Numerical Analysis." NA, KTH. 2011.

[7] Johan Hoffman and Claes Johnson. “Computational Turbulent

Incompressible Flow. Springer, 2006.

[8] A. Ern and J. L. Guermond. “Theory and Practice of Finite Elements." Spriner series: Applied Mathematical Sciences. Springer. Volume-159, 2004.

[9] Santiago Badia, Ramon Codina and Juan Vicente Gutierrez-Santacreu. “Long-term stability estimates and existence of a global attractor in a finite element approximation of the navierstokes equations with numerical subgrid scale modeling." Siam J. Numer. Anal., Volume-48, 2010.

[10] Claes Johnson, Uno Navert and Juhani Pitkaranta. “Finite Element Methods for Linear Hyperbolic Problems." Computer methods in Applied Mechanics and Engineering. Volume-45, 1984.

[11] Peter Hansbo and Anders Szepessy. “A velocity-pressure streamline diffusion finite element method for the incompressible Navier–Stokes equations." Computer methods in Applied Mechanics and Engineering. Volume-84, 1990.

[12] Klaus-Jurgen Bathe. “The inf–sup condition and its evaluation for mixed finite element methods." Computers and Structures. Volume-79, 2001.

[13] P. Sagaut. “Large Eddy Simulation for Incompressible Flows." Springer-Verlag, Berlin, Feidelberg, Newyork. 2001.